Ultrashort pulse characterisation with SHG collinear-FROG

Ivan Amat-Roldán, Iain G. Cormack, Pablo Loza-Alvarez

Ultrafast Imaging Group ,Institut de Ciències Fotòniques, Edifici Nexus-II, c\Jordi Girona, 19 1-D 08034 Barcelona, Spain.
ivan.amat@upc.es

Emilio J. Gualda, David Artigas

Departament de Teoria del Senyal i Communicacions, Universitat Politècnica de Catalunya, Campus Nord, 08034 Barcelona, Spain.

Abstract: We outline criteria for fast and accurate acquisition of collinear FROG (CFROG) trace and how it can be transformed into the more traditional noncollinear FROG trace. The CFROG has an intrinsically simple geometry that provides greater versatility as well as the ability for built-in delay calibration and enhanced error-checking. The procedure, based on data processing, allows conventional SHG-FROG retrieval algorithms to be used. This technique is tested numerically and experimentally giving excellent results. This work represents an attractive alternative to the traditional, more complex non-collinear FROG technique while, at the same time, extending its use to experiments where collinear geometry is imposed.

OCIS codes: (100.5070) Phase retrieval; (190.1900) Diagnostic applications of nonlinear optics; (320.7100) Ultrafast measurements.

References and Links

1. R. Trebino, K. W. DeLong, D. N. Fittinghoff, J. N. Sweetser, M. A. Krumbugel, B. A. Richman, and D. J. Kane, "Measuring ultrashort laser pulses in the time-frequency domain using frequency-resolved optical gating," Rev. Sci. Instrum. **68**, 3277-3295 (1997).
2. A. Baltuska, M. S. Pshenichnikov, and D. A. Wiersma, "Amplitude and phase characterization of 4.5-fs pulses by frequency-resolved optical gating," Opt. Lett. **23**, 1474-1476 (1998).
3. R. Trebino and D. J. Kane, "Using Phase Retrieval to Measure the Intensity and Phase of Ultrashort Pulses - Frequency-Resolved Optical Gating," J. Opt. Soc. Am. A **10**, 1101-1111 (1993).
4. Z. Y. Wang, E. Zeek, R. Trebino, and P. Kvam, "Determining error bars in measurements of ultrashort laser pulses," J. Opt. Soc. Am. B **20**, 2400-2405 (2003).
5. D. N. Fittinghoff, J. A. Squier, C. P. J. Barty, J. N. Sweetser, R. Trebino, and M. Muller, "Collinear type II second-harmonic-generation frequency-resolved optical gating for use with high-numerical-aperture objectives," Opt. Lett. **23**, 1046-1048 (1998).
6. D. N. Fittinghoff, A. C. Millard, J. A. Squier, and M. Muller, "Frequency-resolved optical gating measurement of ultrashort pulses passing through a high numerical aperture objective," IEEE J. Quantum Electron. **35**, 479-486 (1999).
7. I. Amat-Roldán, G. Cormack, P. Loza-Alvarez, and D. Artigas, ""Nonlinear microscopy pulse optimization at the sample plane using Second Harmonic Generation from starch." Proc. SPIE, 5463-09, 2004.
8. J. H. Chung and A. M. Weiner, "Ambiguity of ultrashort pulse shapes retrieved from the intensity autocorrelation and the power spectrum," IEEE J. Selec. Top. Quantum Electron. **7**, 656-666 (2001).
9. D. T. Reid, P. Loza-Alvarez, C. T. A. Brown, T. Beddard, and W. Sibbett, "Amplitude and phase measurement of mid-infrared femtosecond pulses by using cross-correlation frequency-resolved optical gating," Opt. Lett. **25**, 1478-1480 (2000).

#3859 - $15.00 US Received 20 February 2004; revised 16 March 2004; accepted 16 March 2004

10. K. Naganuma, K. Mogi, and H. Yamada, "General-Method for Ultrashort Light-Pulse Chirp Measurement," IEEE J. Quantum Electron. **25**, 1225-1233 (1989).
11. A. Watanabe, H. Saito, Y. Ishida, and T. Yajima, "Computer-Assisted Spectrum-Resolved Shg Autocorrelator for Monitoring Phase Characteristics of Femtosecond Pulses," Opt. Commun. **63**, 320-324 (1987).
12. J. Jasapara and W. Rudolph, "Characterization of sub-10-fs pulse focusing with high-numerical-aperture microscope objectives," Opt. Lett. **24**, 777-779 (1999).
13. J. W. Nicholson, M. Mero, J. Jasapara, and W. Rudolph, "Unbalanced third-order correlations for full characterization of femtosecond pulses," Opt. Lett. **25**, 1801-1803 (2000).
14. L Gallmann, G. Steinmeyer, D. H. Sutter, N. Matuschek, U. Keller, "Collinear type II second-harmonic-generation frequency-resolved optical gating for the characterization of sub-10-fs optical pulses," Opt. Lett. **25**, 269-271 (2000).
15. G. Steinmeyer, "A review of ultrafast optics and optoelectronics," J. Opt. A **5**, R1-R15 (2003).
16. A. V. Oppenheim and R. W. Schafer, *Digital Signal Processing* (Prentice-Hall, 1975).

1. Introduction

Frequency Resolved Optical Gating (FROG) is one of the most common and robust approaches to fully characterise an ultrashort pulse. It has been successfully used to characterise pulses from the UV to the near-infrared [1] with durations of only a few femtoseconds [2]. The FROG technique, can be implemented by exploiting several nonlinear effects such as: Polarization-Gate (PG-FROG), Self-Diffraction (SD-FROG), Transient-Grating (TG-FROG) and Second-Harmonic-Generation (SHG-FROG) [1,3]. Among all of them, SHG-FROG is the most popular because it can exploit the high second order nonlinear coefficient rather than the, generally weaker, third order nonlinearities. SHG-FROG is also, in general, the preferred method for sub-100fs pulse characterization as it introduces very little material dispersion before the non-linear process takes place. A SHG-FROG trace consists of a frequency-resolved SHG intensity autocorrelation that provides the necessary frequency and time information to reconstruct the original intensity and phase of the pulse. It has been shown that such collection of data, besides providing an improved noise immunity [4], has built-in consistency checks via marginal analysis, that allows the detection of different sources of error. Consequently, SHG-FROG techniques offer a complete set of tools to ensure a robust retrieval within a widespread range of cases. Unfortunately, in general, all these approaches are limited for use within a noncollinear geometry (Fig. 1).

Collinear geometry is often imposed in a number of cases where ultrashort pulse characterisation is required [5,6]. For example, pulse optimisation at the sample plane of a nonlinear microscope [7] is required to minimise radiation and maximise the generated nonlinear signal on the biological sample, helping to prolong the specimen's lifetime. Here, a collinear geometry is imposed since the full numerical aperture (NA) of the objective lens has to be fully filled. Measuring an ultrashort pulse under collinear geometry has several difficulties and no general method has yet been reported. Interferometric autocorrelation (IA), which is a collinear technique, is highly sensitive to phase changes, and initial thoughts would assume it to be an excellent way of fully characterising an ultrashort pulse. However, problems exist that limit the use of IA. An example of such a problem is the way that different pulses can in fact produce very similar IA and SHG spectrum [8]. There have been several attempts to find a general method for ultrashort pulse measurement under collinear geometry but normally, a priori knowledge of the pulse is required [9]. An algorithm to retrieve an ultrashort pulse by measuring the interferogram and the IA has been utilised [10] but it has been shown to be susceptible to giving erroneous results under experimental conditions. A computer assisted spectrum-resolved SHG autocorrelator for monitoring phase characteristics was also proposed [11]. The IA has been used to measure the pulse width of sub-10-fs pulse passing through a microscope objective by assuming a Group Delay which is radius-dependent [12]. This technique however is not a direct pulse measurement and is susceptible to experimental errors that occur within both the characterization of the objective lens as well as the pulse measurement before the objective lens. Finally, an unbalanced third-order cross-correlation has been used to fully characterize ultrashort pulses by using another algorithm

#3859 - $15.00 US Received 20 February 2004; revised 16 March 2004; accepted 16 March 2004

(PICASO) [13]. Although PICASO is perhaps the most successful of all IA techniques described here it is however, as with all of the IA techniques, lacking the essential error checking ability that FROG possesses and as a consequence will always be susceptible to experimental error. Thus, several attempts have been performed to obtain a FROG trace using a collinear geometry [5,6] by way of type II SHG signals. These techniques include the incorporation of λ/2 plates into one arm of the autocorrelator to cross polarize the beams so that the interferfeometric fringes are eliminated. This technique however, may be unappropriate when dealing with very short pulses (< 20 fs), as it adds extra dispersion by way of the λ/2 plates. More recently, this problem was solved by introducing a periscope for polarization rotation inside the autocorrelator [14] but at the expenses of adding complexity to the technique. In this paper we report a general process to convert an SHG-based collinear FROG (SHG-CFROG) trace into a conventional noncollinear SHG-FROG trace. This allows the use of well established algorithms while at the same time, eliminating the problems that the previous approaches had.

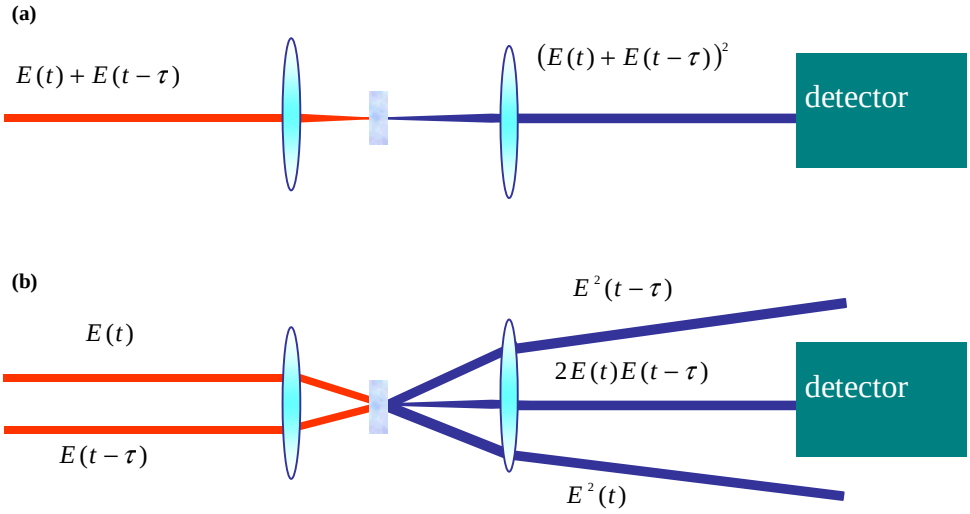

Fig. 1. Schematic representing the differences within the detected (a) collinear and (b) noncollinear signal.

This paper is organized as follows. In section two we present the analytical expression for the collinear detection. In section three, a pre-processing technique which properly retains the embedded SHG-FROG information is presented. A simulation tool is then used to test out analytical results and to help draw attention to some of the extended advantages that this technique has, such as built-in error checking and self-calibration of the axis. In section four, we present an experimental comparison of a fully-filtered SHG-CFROG trace with a classically obtained noncollinear SHG-FROG trace. Finally, in section five, we summarize our main conclusions.

2. Theory

The purpose of this section is to analytically show that the SHG-FROG trace is embedded into the SHG-CFROG trace. A general method is then outlined to unwrap the desired FROG information and used to demonstrate additional features of the collinear geometry approach.

We define the complex electric fields as

$$\hat{E}(t) = E(t)\exp\left(j2\pi f_0 t\right) \qquad (1)$$

#3859 - $15.00 US Received 20 February 2004; revised 16 March 2004; accepted 16 March 2004

where $E(t)$ is the slowly-varying amplitude and f_0 is the optical carrier. The quadratic response of two pulses interacting in a nonlinear medium is given by

$$\left(\hat{E}(t)+\hat{E}(t-\tau)\right)^2. \tag{2}$$

When using the noncollinear geometry, it is experimentally possible to retain only the information of the required cross-term, see Fig. 1, given by:

$$\hat{E}(t)\hat{E}(t-\tau). \tag{3}$$

The SHG-FROG trace is an intensity autocorrelation that has been frequency-resolved and sampled within a delay-frequency grid. Thus, its general expression as a function of the input pulse $E(t)$, is obtained using Eq. (2) as [1,3,15]

$$I_{FROG}^{SHG}(\tau, f) \propto \left| \int_{-\infty}^{\infty} \hat{E}(t)\hat{E}(t-\tau)\exp(-j2\pi ft)dt \right|^2 \tag{4}$$

This expression, however, does not apply for a collinear geometry. Thus, in order to obtain a general expression of the CFROG trace we need to substitute in Eq. (4) not the quadratic response of the noncollinear geometry, Eq. (3), but that of the collinear geometry, that is directly given by Eq. (2):

$$I_{CFROG}^{SHG}(\tau, f) \propto \left| \int_{-\infty}^{\infty} \left(\hat{E}(t)+\hat{E}(t-\tau)\right)^2 \exp(-j2\pi ft)dt \right|^2 \tag{5}$$

Its is clear from this expression that the CFROG trace resolves, in frequency, the whole quadratic response of the medium, given by Eq. (2). Fringes therefore appear due to diverse electric fields interfering with one another. By expanding the above expression it is possible to establish the relations between the FROG trace and the collinear approach. The collinear term, Eq. (2), can be grouped in three major terms: $E^2(t)$, which represents the pulse interacting with itself; $E^2(t-\tau)$, which represents the delayed pulse interacting with itself; and $E(t)E(t-\tau)$, the cross term, which represents the pulse interacting with the delayed pulse. By Fourier analysis, Eq. (5) can be written as the addition of four terms occurring at different delay-frequencies:

$$\begin{aligned} I_{CFROG}^{SHG}(\tau, f) \propto \quad & 2I_{SHG}(f) \\ & + \quad 2I_{SHG}(f)\cos\left(2\pi(2f_0+f)\tau\right) \\ & + \quad 4\mathrm{Re}\left\{E_{SHG}^{*}(f)E_{FROG}^{SHG}(\tau, f)\left(\exp(-j2\pi f_0\tau)+\exp(j2\pi(f_0+f)\tau)\right)\right\} \\ & + \quad 4I_{FROG}^{SHG}(\tau, f) \end{aligned} \tag{6}$$

in which

$$E_{SHG}(f) \propto \int_{-\infty}^{\infty} E^2(t)\exp(-j2\pi ft)dt \tag{7}$$

#3859 - $15.00 US Received 20 February 2004; revised 16 March 2004; accepted 16 March 2004

where $I_{SHG}(f) \propto \left|E_{SHG}(f)\right|^2$, and

$$E_{FROG}^{SHG}(\tau, f) \propto \int_{-\infty}^{\infty} E(t)E(t-\tau)\exp(-j2\pi ft)dt \qquad (8)$$

where $I_{FROG}^{SHG}(f) \propto \left|E_{FROG}^{SHG}(f)\right|^2$.

The two first terms in Eq. (6) correspond to the intensity resulting from the linear interference between the SHG of the pulse and the delayed one. In particular, the first term, corresponding to the SHG intensity of both the delayed and non-delayed pulses, is related with the inherent background in an IA. The second term contains the exact same background information but modulated by $2f_0$ in the delay-frequencies and is the cross term of the interference between the two SHG pulses. The third term, modulated at f_0 is obtained from the interaction between the SHG field given by Eq. (3) and the SHG of the two individual pulses. Finally, the last term carries the SHG-FROG information. This last term is exactly the same as the measured under noncollinear conditions, and thus needs to be unwrapped for our purposes. The next section describes a technique to unwrap the SHG-FROG term from the other terms.

3. Simulation

The previous analysis shows that the noncollinear trace term is embedded within the collinear one. Within this section we show by using a simulation tool that it is possible to unwrap the noncollinear term. By carrying out this analysis we have verified the integrity of the procedure helping to show important properties associated with the collinear approach.

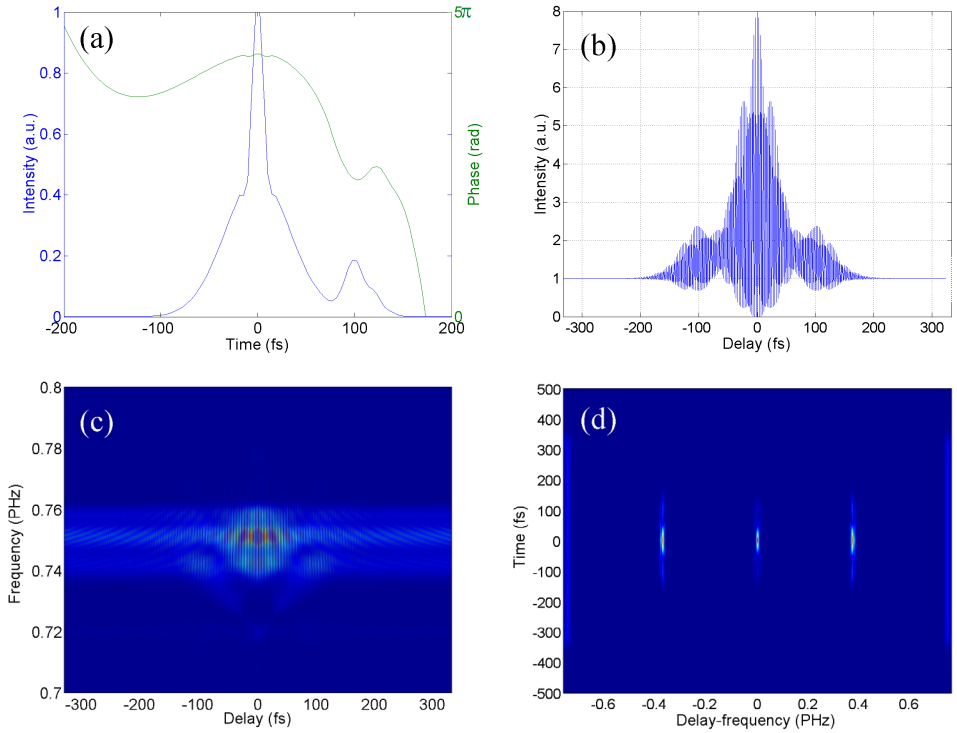

Fig. 2. Numerical results: (a) Multiple-pulse with cubic phase employed as input in our simulation tool (b) Interferometric Autocorrelation (c) CFROG trace (d) Fourier Transformed CFROG trace.

#3859 - $15.00 US Received 20 February 2004; revised 16 March 2004; accepted 16 March 2004

Figure 2(a) illustrates a pulse of Δt = 25 fs (measured at FWHM) showing an arbitrary shape and phase. Figure 2(b) shows its IA and in Fig. 2(c) the resulting CFROG trace with a delay sampling according to the Nyquist limit [16]. It is important to notice that to resolve the interferometric fringes the sampling must be at a delay step $\Delta\tau_N < 1/2f_{max} = 1/4f_0$. Before going further, we have to realise that a CFROG trace is an IA that has been frequency-resolved. Therefore, by integrating the spectrogram shown in Fig. 2(c) in frequency it is possible to recover the autocorrelation shown in Fig. 2(b). This allows the characteristic 8:1 ratio of an IA to be verified during acquisition, providing a simple method to check the integrity of the measured trace in the laboratory. Additionally, the delay axis can be self calibrated by measuring the fringes. This enhances the detection of errors during the experimental measurement while, at the same time, helping add consistency to the acquired results.

To enable the unwrapping of the noncollinear FROG term we should notice that the second and third terms in Eq. (6), are modulated at frequencies f_0 and $2f_0$. These two terms can be removed by low pass band Fourier filtering. Fast Fourier transforming (FFT) a CFROG trace assumes periodicity in the applied direction. This is a condition which is impractical to carry out when experimentally acquiring the trace. As a consequence, an error will be introduced in the form of modulation components in the frequency direction. By using a two-dimentional Fourier Filter this error is greatly reduced. Figure 2(d) reveals the two-dimensional Fourier Transform of the SHG-CFROG trace. It can be seen from this figure that a relaxed cut-off frequency for filtering can be applied without major loss of information since the interferometric terms f_0 and $2f_0$ are well separated from the DC. After filtering, the first term in Eq. (6) is the only non-desired term remaining in the CFROG trace. This term, the SHG spectrum, overlaps with the DC term. It can either be measured or averaged from several samples at the edges of the delay axis and subtracted from the trace. After all this process, the remaining DC term contains the same information as a noncollinear SHG-FROG trace and thus a normal retrieval algorithm can be employed. Figure 3(a) and (b) show the filtered CFROG trace and the numerically generated non-collinear FROG trace, respectively. An excellent agreement between both traces can be observed. This is confirmed with an RMS G-Error between the two traces being $G = 2.7 \cdot 10^{-7}$. Finally, the need of a two-dimensional filtering is highlighted by comparing this result with that obtained when using a one-dimensional Fourier filtering. In this case, a much larger G-Error (G_{1D}), is obtained, having a value of $G_{1D} > 10^{-2}$.

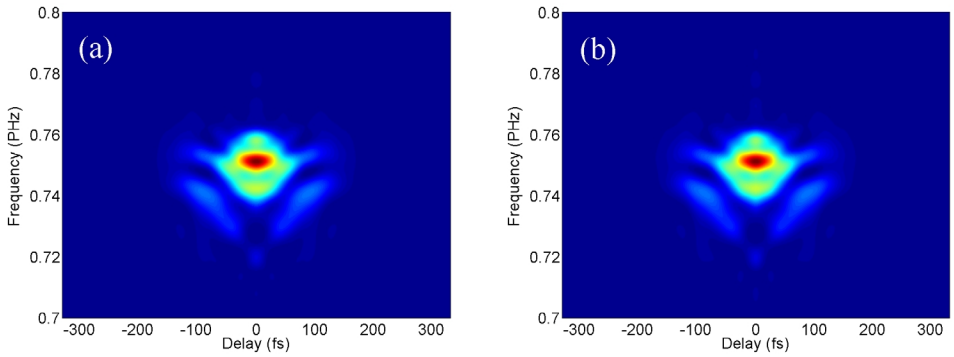

Fig. 3. Numerical results: (a) filtered CFROG trace (b) FROG trace. $G=2.7 \cdot 10^{-7}$.

This simulation has shown that it is possible to obtain SHG-FROG traces under collinear geometry for complex pulses. This allows for full pulse characterization for a broader range of cases hence, extending the usefulness of the FROG technique. This includes the possibility of characterising very short pulses (Δt < 20 fs) using a type I SHG phasematching. It should also be noted that when dealing with such short pulses, just a few points are required when

#3859 - $15.00 US Received 20 February 2004; revised 16 March 2004; accepted 16 March 2004

sampling at the Nyquist limit and, as a consequence, it is possible to acquire the trace quickly. For example, obeying Nyquist, a Ti:Sap laser at 800nm will require a delay step of $\Delta\tau_N < 0.66$ fs. For unchirped 10 fs pulses only about 80 data points are needed. However, for pulses that include a large number of optical cycles, i.e. 100-fs, over 800 data points would have to be acquired. This, therefore, generates a large and clumsy data set which is both difficult and time consuming to acquire and analyse.

The possibility to overcome the Nyquist limit will result in a faster measurement. To do this, we need to realize that we do not need to resolve the interferometric fringes as the algorithm only uses the DC term. If however undersampling is carried out both the acquisition and data processing time can be significantly reduced without major loss in accuracy. In what follows we will describe a methodology to carry out this undersampling.

We must first notice that the use of undersampling in the delay-frequency (or k-domain) causes frequencies above the Nyquist limit (B_N) to shift to lower frequencies [16]. For instance, a component $k > B_N$, will be shifted to a new frequency given by:

$$k' = k - n \cdot k'_{span} \tag{9}$$

where n is an integer and $k'_{span} = 1/\Delta\tau$ is the total span of the k'-domain.

In order to measure an undersampled CFROG trace capable of successful filtering we consider two constraints. The first constraint is to choose an appropriate delay step ($\Delta\tau$) to avoid frequency overlapping of the interferometric terms with the DC-FROG component. To achieve this, the shifted frequencies must be as far away as possible from the DC term ($k'=0$). From Eq. (9), it is possible to demonstrate that this optimal situation occurs when f_0 is shifted to $\pm k'_{span}/3$ and $2f_0$ to $\mp k'_{span}/3$. Given this, the optimum delay step is:

$$\Delta\tau = \frac{n \pm \frac{1}{3}}{f_0} \tag{10}$$

Even if the condition in Eq. (10) is satisfied, overlapping of the delay-spectral components can still occur for very large undersampling. To avoid this from happening, we need to ensure that the delay step in Eq. (10) is not too large, thus the following restriction needs to be imposed:

$$\Delta\tau < \frac{\tau_{IA}}{10} \tag{11}$$

where τ_{IA} is defined as the full width at 15% of the maximum of the IA trace. This condition is equivalent to using more that 10 samples within the trace envelope. For simple well behaved bell-shaped pulses, this condition has been proven to work fine without loss of accuracy. However, to retain high frequency components within more complex pulses, a larger number of sampling points may be required.

The second constraint is used to define a sufficient delay span τ_{span} to give negligible error:

$$\tau_{span} = \frac{1}{\Delta k} \geq 2 \cdot \tau_{IA} \tag{12}$$

From Eq. (11-12), we see that a minimum of 20 samples is required.

In summary, the use of Eq. (10) with the restriction in Eq. (11) ensures that the distribution of the interferometric terms are sufficiently far away from DC term. In addition, Eq. (12) helps define a sufficient delay span for an accurate acquisition. Thus, a flexible and robust undersampling criterion is proposed which allows for fast-CFROG acquisition.

#3859 - $15.00 US Received 20 February 2004; revised 16 March 2004; accepted 16 March 2004

3. Experimental comparison

To further test this technique, we compared two experimentally acquired traces. One trace was obtained as a conventional noncollinear FROG trace while the other one was obtained by filtering an undersampled CFROG trace. Both traces were obtained from the same laser source during a single experiment.

The pulses from a Kerr-lens mode-locked Ti:Sapphire laser with average power of 1.5 W, a wavelength of 800nm and a repetition rate of 76 MHz were focused into an SHG type I BBO crystal through an autocorrelator. The SHG signal was sent to a spectrograph and detected by a CCD linear array. This arrangement enabled us to obtain a SHG-FROG trace and SHG-CFROG trace under very similar conditions. The delay step of the CFROG trace was fixed at $\Delta\tau = 1.76$ *fs*, and it was estimated that $\tau_{IA} \approx 450$ fs (thus $\tau_{span} = 900$ fs). We first collected the data under a collinear geometry. Figure 4 shows (a) the collinear measurement and (b) the two-dimensional Fourier Transform of it. Also, in Fig. 4(c), we plot the IA obtained by integrating the CFROG trace showing that the characteristic 8:1 ratio can be checked even under undersampling conditions.

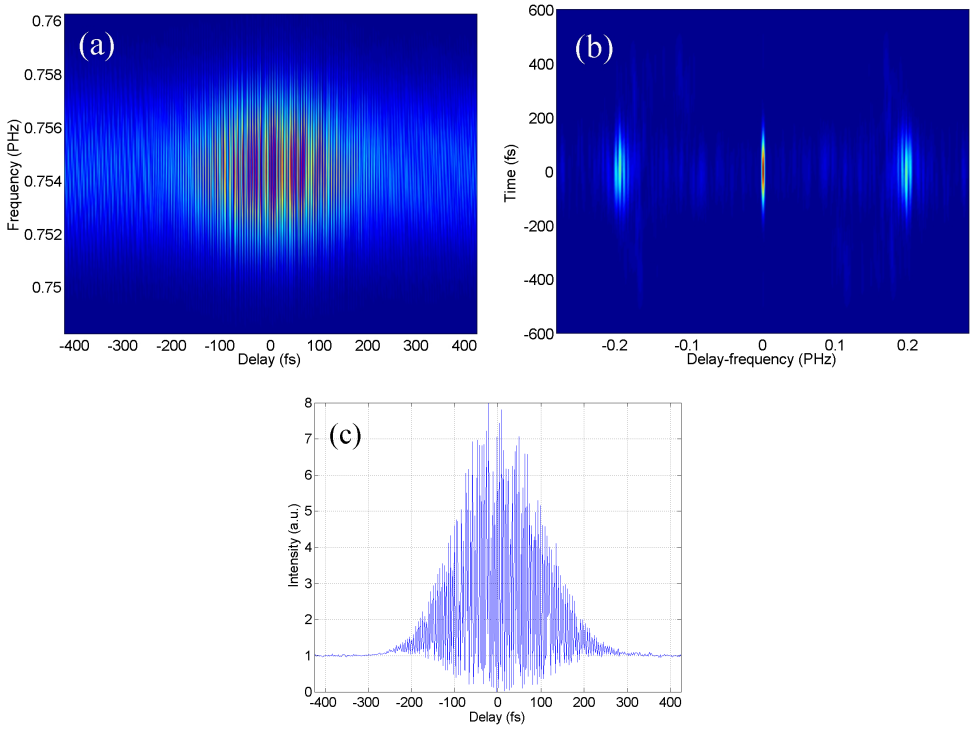

Fig. 4. (a) Measured CFROG, (b) fourier transformed CFROG and (c) measured IA with a delay step of 1.76 fs and 512 samples.

We then proceeded to perform the background subtraction and Fourier filtering to the CFROG trace. The fully filtered CFROG trace can be seen in Fig. 5(a). Without stopping the laser, we changed to a noncollinear geometry. The resulting FROG trace is shown in Fig. 5(b).

#3859 - $15.00 US Received 20 February 2004; revised 16 March 2004; accepted 16 March 2004

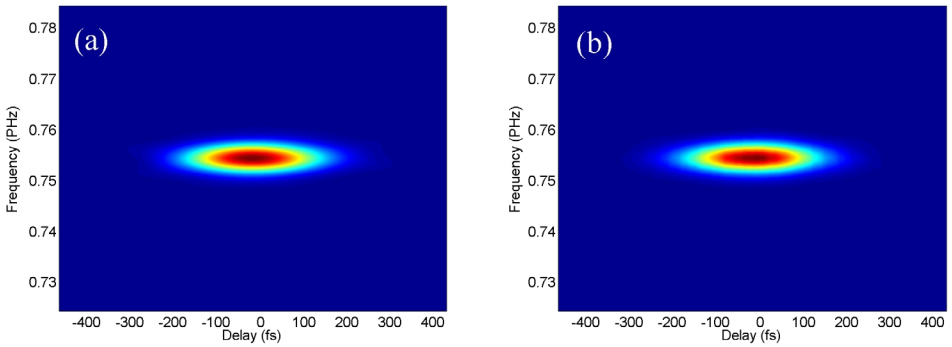

Fig. 5. (a) filtered fast-CFROG trace and (b) FROG trace. $G=3.9\cdot10^{-6}$.

We demonstrated the effectiveness of this technique by comparing both traces and computing the G. For this reason, it was necessary to interpolate the FROG trace to obtain the same delay step of 1.76 fs. Excellent agreement is observed between the two traces (Fig. 5), where $G = 3.1\cdot10^{-5}$. To further check this result, time and frequency marginals for both traces have been calculated. Figure 6 shows a comparison of such marginals where again very good agreement is obtained.

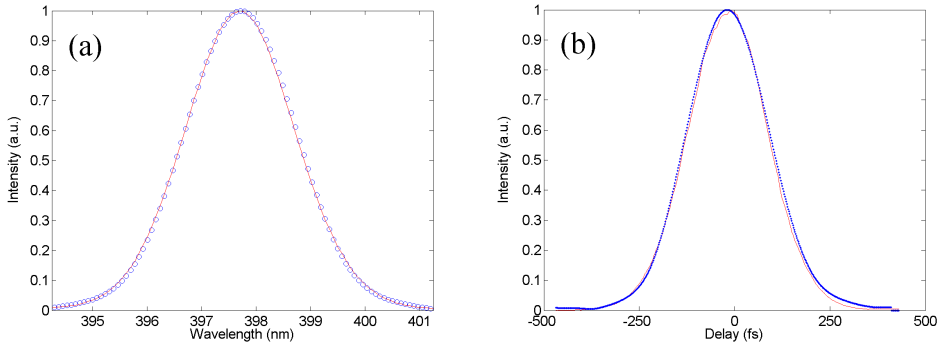

Fig. 6. (a) Marginal of the spectrum from the filtered CFROG trace (blue circles) and FROG trace (red line); (b) Intensity autocorrelation (delay marginal) from the filtered CFROG trace (blue dots) and the FROG trace (red line).

From the above figure, we can confirm that both traces are equivalent and that running the FROG retrieval algorithm with any of the traces shown in Fig. 5, will retrieve the same pulses.

In order to investigate the effect of undersampling has upon the experimentally acquired CFROG trace, we proceeded to resample our CFROG trace in Fig. 4(a) to a lower number of points (N). Thus traces of N = 256, 128, 64, 32 and 16 samples were generated from the original (N = 512 sampled) trace. This is equivalent to increase the $\Delta\tau_1$ in powers of two for each case. Even for the highest sampling rate (N = 16), we obtained a relatively low error of $G = 1.6\cdot10^{-3}$. This sampling rate is below our sampling limit (Eq. (10-12)), but as previously mentioned, for well-behaved pulses our criteria may be relaxed.

4. Conclusions

In this paper we have reported the application of a pre-processing technique that allows a SHG-FROG retrieval algorithm to be utilized from a trace that has been measured under collinear conditions. This allows for more flexible, easier and multipurpose experimental conditions that reduce the overall experimental constraints of the FROG technique while at

#3859 - $15.00 US Received 20 February 2004; revised 16 March 2004; accepted 16 March 2004

the same time helping to broaden the number applications in which FROG measurements can be utilized, e.g., nonlinear microscopy pulse optimisation. The preprocessing technique based on a filtering and background subtraction procedure has been analytically justified. The robustness of our approach has been fully tested using both numerical simulations and experimental data. In both cases, excellent agreement has been observed between the filtered CFROG trace and the noncollinear FROG trace. In the case of an experimental trace, a G-Error of $G \leq 10^{-5}$ was obtained. Furthermore, we have shown that, as the technique does not rely on resolving the interferometric fringes, it is possible to significantly reduce the acquisition time by undersampling the CFROG trace. A standard procedure is then presented to minimize the number of samples while ensuring little error is introduced into the trace.

We have focused upon SHG-FROG based measurements, but in a similar manner, this method can be extended to other FROG geometries. The result is a general method for full characterisation of ultrashort pulses under collinear conditions.

Acknowledgments

This work was supported by the Generalitat of Catalunya, the Spanish Government under grant TIC2003-07485 and by the European Regional Development Fund. P. Loza-Alvarez acknowledges funding from the Spanish Government through the Ramón y Cajal program.

#3859 - $15.00 US Received 20 February 2004; revised 16 March 2004; accepted 16 March 2004